AIP Proceedings

Microwave-based laboratory experiments for internally-heated mantle convection

A. Limare, E. Surducan, V. Surducan, C. Neamtu, E. di Giuseppe, K. Vilella, C. G. Farnetani, E. Kaminski, and C. Jaupart

Citation: AIP Conference Proceedings **1565**, 14 (2013); doi: 10.1063/1.4833687
View online: http://dx.doi.org/10.1063/1.4833687
View Table of Contents: http://scitation.aip.org/content/aip/proceeding/aipcp/1565?ver=pdfcov
Published by the AIP Publishing

This article is copyrighted as indicated in the abstract. Reuse of AIP content is subject to the terms at: http://scitation.aip.org/termsconditions. Downloaded to IP: 194.254.220.140 On: Tue, 19 Nov 2013 08:34:07

Microwave-based laboratory experiments for internally-heated mantle convection

A. Limare*, E. Surducan†, V. Surducan†, C. Neamtu†, E. di Giuseppe*, K. Vilella*, C. G. Farnetani*, E. Kaminski* and C. Jaupart*

*Institut de Physique du Globe de Paris, Sorbonne Paris Cité, Université Paris-Diderot, CNRS, 1 rue Jussieu, F-75005 Paris, France

†National Institute for Research and Development of Isotopic and Molecular Technologies, 65-103 Donath, 400293 Cluj-Napoca, Romania

Abstract. The thermal evolution of terrestrial planets is mainly controlled by the amount of radioactive heat sources in their mantle, and by the geometry and efficiency of solid state thermo-chemical convection within. So far, these systems have been studied using numerical methods only and cross validation by laboratory analogous experiments has not been conducted yet. To fill this gap we perform the first laboratory experiments of mantle convection driven by microwave-generated internal heating. We use a 30x30x5 cm^3 experimental tank filled with 0.5 % Natrosol in water mixture (viscosity 0.6 Pa.s at 20°C). The fluid is heated from within by a microwave device that delivers a uniform volumetric heating from 10 to 70 kW/m^3; the upper boundary of the fluid is kept at constant temperature, whereas the lower boundary is adiabatic. The velocity field is determined with particle image velocimetry and the temperature field is measured using thermochromic liquid crystals which enable us to charaterize the geometry of the convective regime as well as its bulk thermal evolution. Numerical simulations, conducted using Stag-3D in 3D cartesian geometry, reproduce the experimental setup (i.e., boundary conditions, box aspect ratio, temperature dependence of physical parameters, internal heating rate). The successful comparison between the experimental and numerical results validates our approach of modelling internal heating using microwaves.

Keywords: mantle convection, microwave heating
PACS: <44.25+f, 91.35.Dc, 41.20Jb>

INTRODUCTION

The thermal evolution of rocky planets is controlled by the efficiency of solid state thermal convection within their mantles, which is driven by both internal heating and heating from below. For terrestrial planets, cooling and solidification of the iron-rich core is the primary source of heating from below, and the heat flux out of the core accounts for about one third of the heating source in the Earth [1]. Volumetric heating, due to radioactive decay of ^{238}U, ^{235}U, ^{232}Th and ^{40}K in the mantle, represents the main source of heating within the Earth [2]. Many issues remain to be solved to get a complete and quantitative understanding of convection in the Earth's mantle. In particular, intrinsic chemical heterogeneities in planetary bodies imply large heterogeneities in the distribution of internal sources that shall significantly affect thermal convection, which in turn controls the rate of creation and destruction of chemical heterogeneities in the system [3, 4, 5]. Geological data remain too scarce to fully constrain the evolution of such a nonlinear system, especially during the early stages of the planet, and combined numerical and experimental modelings are essential tools.

Thermal convection in a heterogeneous system heated from within has not been studied experimentally due to numerous technical difficulties. In the few experimental studies published so far, the heat sources are produced by the ohmic dissipation of an electric current passed through an electrolyte fluid layer [6, 7]. Most works were restricted to aqueous solutions i.e. small Prandtl (Pr) number, whereas Pr is considered infinite in rocky planets [8, 9]. It has been demonstrated [10, 11] that thermal convection in a plane layer of fluid with uniformly distributed heat sources between boundaries at constant temperatures is equivalent to thermal convection in a plane layer of fluid with boundary temperatures that are spatially uniform but decrease in time at constant rate. This technique is simpler and more flexible than the electrolytic one and enables to mimic a system heated from below and internally. However, this artifice cannot be applied to temperature dependent viscosity liquids and cannot produce high Rayleigh numbers appropriate for planetary convection.

To overcome the limitations of previous studies, we propose an original mode of internal heating produced by microwave (MW) absorption. Microwave heating (MWH) potentially provides a very efficient way of producing non-contact, localised or extended heat sources by a convenient choice of microwave antenna, excitation sequence and selective absorption of fluids [12, 13]. Here we present the first experimental results obtained using a

Processes in Isotopes and Molecules (PIM 2013)
AIP Conf. Proc. 1565, 14-18 (2013); doi: 10.1063/1.4833687
© 2013 AIP Publishing LLC 978-0-7354-1193-7/$30.00

This article is copyrighted as indicated in the abstract. Reuse of AIP content is subject to the terms at: http://scitation.aip.org/termsconditions. Downloaded to IP: 194.254.220.140 On: Tue, 19 Nov 2013 08:34:07

specifically designed MW prototype. The experimental results are compared with numerical simulations, conducted with the code Stag-3D [14] in 3D cartesian geometry, thereby providing the first cross validation of experimental and numerical studies of convective viscous systems heated from within.

EXPERIMENTAL DESIGN

In the classical Rayleigh-Bénard framework, thermal convection in an isoviscous fluid is characterized by two dimensionless parameters, the Rayleigh number and the Prandtl number. The Rayleigh number, *Ra*, is the ratio of the driving thermal buoyancy forces over the thermal and viscous dissipation:

$$Ra = \frac{\rho g \alpha \Delta T h^3}{\kappa \mu} \tag{1}$$

where ρ is the density, g the gravitational constant, α the thermal expansion coefficient, ΔT the temperature difference between the top and bottom of the layer, κ the thermal diffusivity, μ the dynamic viscosity and h the tank height.

Convection starts when *Ra* exceeds a critical value [15], and follows a sequence of transitions toward chaos as *Ra* increases. The second parameter, the Prandtl number, is defined as the ratio of momentum diffusivity over heat diffusivity:

$$Pr = \frac{\nu}{\kappa} \tag{2}$$

where $\nu = \mu/\rho$ is the kinematic viscosity.

When $Pr \gg 1$ (i.e., inertial effects are negligible compared to viscous effects) the fluid motion stops as soon as the heat source disappears. This is the case for the Earth mantle, where $Pr > 10^{23}$. In practice the use of fluids with $Pr > 100$ is adequate to ensure the dominance of viscous over inertial effects [16].

In the case of purely internally heated case, the Rayleigh number is defined as function of another temperature scale, related to the internal heating rate:

$$\Delta T_h = \frac{H h^2}{\lambda} \tag{3}$$

where λ is the thermal conductivity, and H is the heat generated per unit volume. The resulting number is also called Rayleigh-Roberts number:

$$Ra_H = \frac{\rho g \alpha H h^5}{\lambda \kappa \mu} \tag{4}$$

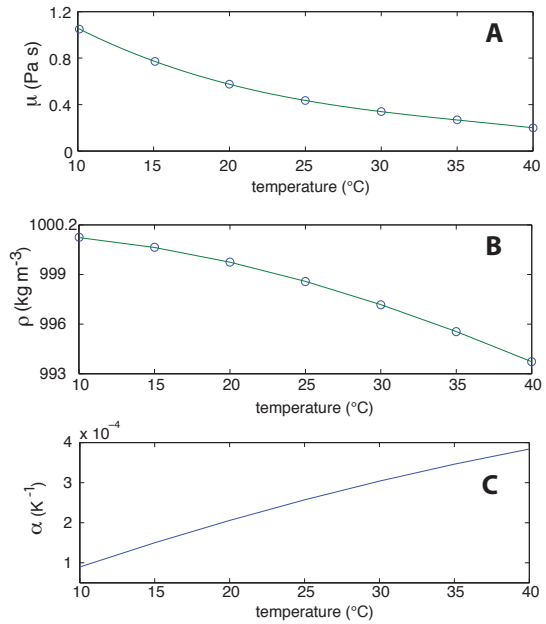

FIGURE 1. Fluid properties as a function of temperature: A: viscosity μ, B: density ρ, C: thermal expansion coefficient α.

Experimental fluids

Rayleigh numbers relevant to mantle convection (10^6-10^8) can be obtained experimentally either by using a low viscosity fluid or by increasing the heat generated per unit volume H (see eq.4). Prandtl numbers larger than 100 can be obtained only if the viscosity is few orders of magnitude larger than water viscosity. Since too low viscosity would imply too low *Pr* number, high H values are required, meaning that the experimental fluids should have water-like, strong MW absorption [17] and that the heating power should reach 300 W (H = 70 kW/m^3).

To obtain such properties we use thickeners such as Hydroxy-ethylcellulose (trade name Natrosol), since by adding a few % of thickener, the viscosity of water can be multiplied by a factor up to 10^7. Although the resulting fluid is shear-thinning, there is a Newtonian plateau at the low shear rates that are typically obtained in convection laboratory experiments [18]. The fluid rheology was characterized with a Thermo Scientific Haake rheometer RS600. Within the Newtonian regime, the viscosity depends on temperature, as shown in Fig.1A. The density of the fluid (Fig.1B) was measured with a DMA 5000 Anton Paar densimeter. The thermal expansivity (Fig.1C) was calculated by polynomial fitting of the density curve.

This article is copyrighted as indicated in the abstract. Reuse of AIP content is subject to the terms at: http://scitation.aip.org/termsconditions. Downloaded to IP: 194.254.220.140 On: Tue, 19 Nov 2013 08:34:07

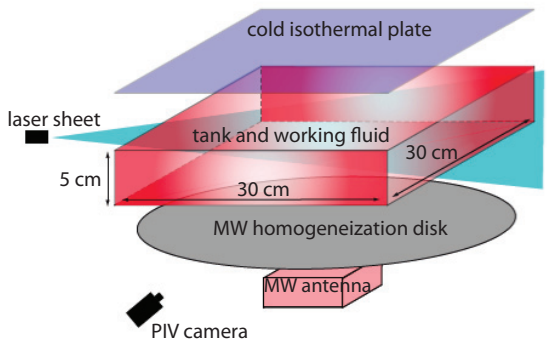

FIGURE 2. Experimental setup.

Experimental setup

The experimental setup is schematically shown in Fig. 2. The MW prototype includes a power MW generator driven by an embedded system, a circuit and an applicator system (antenna) through which the MW radiation propagates towards the working fluid. More details about the MW optimisation in terms of homogeneity of the heating and long-term power stability are given in a related paper [19] presented in this conference. The volumetrically heated fluid is cooled from above with a heat exchanger made of Aluminum, that is temperature-controlled by a thermostatic bath. The tank (30x30x5 cm^3) is made of poly(methyl methacrylate), so the bottom boundary is as close as possible to adiabatic. The experimental tank can be scanned with a laser sheet and the scattered light is registered by a CCD E-lite camera (1.4 Mpixels, 17 Hz) from LaVision.

In the example detailed below, the top of the tank was cooled by a thermostatic bath at 17.2°C. The absorbed power was 102 W, i.e. the generated heat per volume is H = 22.7 kW/m^3. The resulting Rayleigh and Prandtl numbers were $Ra_H = 0.6\text{x}10^6$ and $Pr = 2800$, respectively.

The use of thermochromic liquid crystals (TLC) allows temperature mapping on a 2D-plane in the fluid flow without perturbing it (see [20] for a review). The experimental cell was seeded with several types of TLCs, and a monochromatic laser light sheet was used to illuminate a cross-section of the tank (see Fig.2). Each type of TLC produces one bright line, which represents an isotherm [21]. The fluid was also seeded with small hollow glass spheres that can be considered as passive tracers. Images were taken every 1s, and the velocity field was calculated through cross-correlations between images, using PIV package DaVis from LaVision. The same camera was used for both the temperature and velocity fields.

RESULTS AND DISCUSSION

The thermal structure, as revealed by the isotherms (Fig.3A) shows that convection driven by internal heating is characterised by the formation of several cold plumes from the top, cold, boundary layer. The velocity field (Fig.3B) and the detailed vertical component (Fig.3C) show that cold plumes are associated with downwards velocity zones and that upwards velocity zones are only due to return flow. The images containing the isotherms were used to calculate the temperature field over the entire cross-section by interpolation. The resulting 2D temperature cross-sections, obtained at different laser positions (scanning zone from 10 to 100 mm, one third of the tank), were averaged horizontally. Fig.5 shows the resulting mean temperature curve as a function of tank height, as well as the minimum and the maximum dispersion limits over the scanned zone.

Numerical simulations were performed using Stag3D [14] in 3D cartesian geometry, with 0.6 mm spatial resolution, and we implemented the same conditions (i.e., boundary conditions, box aspect ratio), and the same physical properties (i.e. temperature dependence of physical parameters, internal heating rate) as in the laboratory experiments. Fig.4 shows the 3D temperature field, once the calculation reached the steady-state.

To compare numerical and experimental results, the numerical temperature field was averaged over the lateral dimensions and expressed as a function of the tank height (Fig.5). The maximum dispersion around the mean value is 12% for the simulations and 13% for the experiments. The two experimental and numerical curves present important similarities: i.e. sub-adiabatic behaviour, same mean steady-state temperature increase with respect to the surface temperature (10.04 and 10.02°C for the experimental and numerical curves, respectively). The two curves have identical steady-state heat flux at the top surface (1132 W/m^2), which is a trivial result since the input for the numerical simulation was the experimental value of the internal heating rate. At steady state the total heating power P is equal to the heat flux integrated over the surface (ϕ S).

The small apparent deviation from the adiabatic condition for the experimental temperature curve can be explained by the fact that the experimental temperature field is obtained by interpolation of some discrete values given by the TLCs.

The good agreement between experiments and numerical simulations is also found when analyzing the velocity field. In particular, we can determine the number of cold instabilities from the vertical velocity field by defining an instability as a zone with negative velocities of magnitude larger than the rms value. The average number of instabilities over the tank lateral dimension is about 4 for both the experimental and numerical cases. The insta-

This article is copyrighted as indicated in the abstract. Reuse of AIP content is subject to the terms at: http://scitation.aip.org/termsconditions. Downloaded to IP: 194.254.220.140 On: Tue, 19 Nov 2013 08:34:07

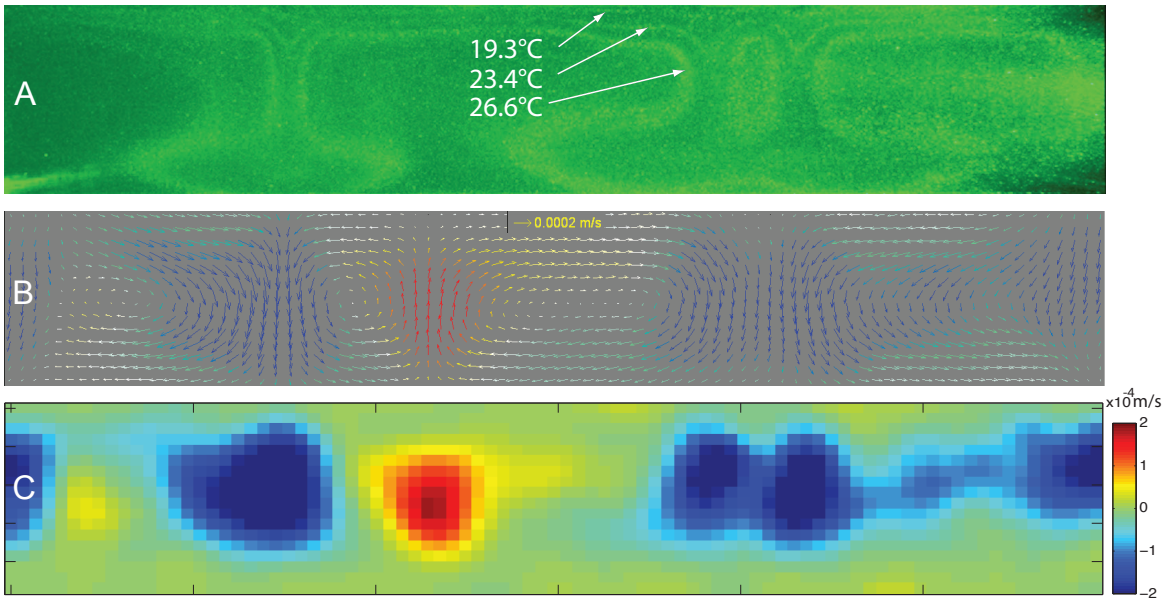

FIGURE 3. A: isotherms, B: velocity field, C: vertical velocity

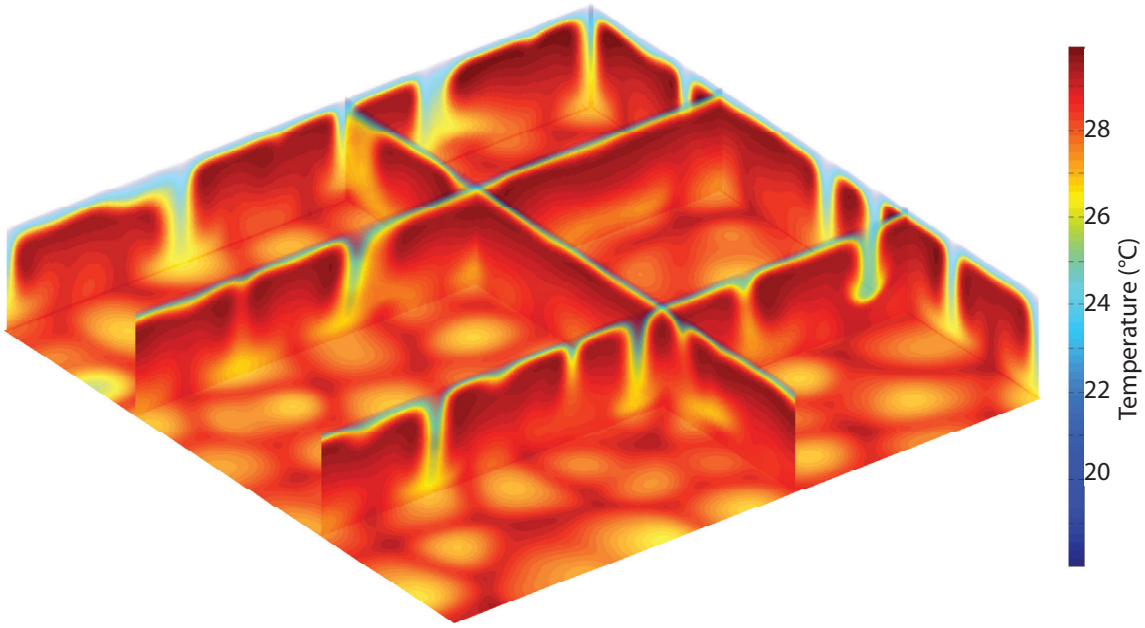

FIGURE 4. Numerical simulation of the 3D temperature field, same conditions as the experiment.

This article is copyrighted as indicated in the abstract. Reuse of AIP content is subject to the terms at: http://scitation.aip.org/termsconditions. Downloaded to IP: 194.254.220.140 On: Tue, 19 Nov 2013 08:34:07

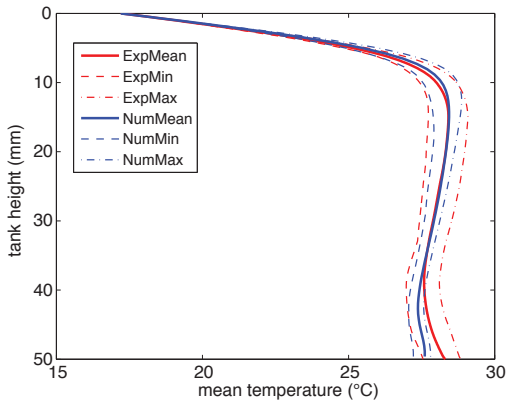

FIGURE 5. Mean temperature over the tank height (red: experimental; blue: numerical). The dashed curves show the minimum and the maximum limits of the temperatures curves to illustrate the dispersion.

bilities "wavelength", measured as the mean distance between two neighbour instabilities is about 75 and 70 mm for the experimental and numerical cases, respectively.

CONCLUSION

The successful comparison between experimental and numerical results shows that we have been able to overcome challenging technological issues inherent with the generation of a uniformly internally heated fluid and with the ability to accurately quantify the temperature and velocity fields during the experiment.

We consider this as a first and necessary step before introducing further complexities, such as bottom heating (to mimic heat flux from the core into the mantle) and compositional heterogeneities (to mimic portions of the mantle variably enriched/depleted in heat producing elements).

Thermal evolution of planets is modelled using scaling laws relating the surface heat flux to the Rayleigh number. These scaling laws, determined numerically, show a large variability. Here we detain for the first time a combination of experimental and numerical methods that will hopefully help us to better constrain the thermal history of the Earth and related planets.

ACKNOWLEDGMENTS

The present work was financed by ANR-11-IS04-0004 (French team) and 1 RO-FR-22 (Romanian team). We thank Anne Davaille and two anonymous reviewers for thorough and constructive reviews.

REFERENCES

1. G. Schubert, D. Turcotte, and P. Olson, *Mantle convection in the Earth and Planets.*, Cambridge University Press, Cambridge, 2001.
2. C. Jaupart, S. Labrosse, and J.-C. Mareschal, “Temperatures, Heat and Energy in the Mantle of the Earth,” in *Treatise of Geophysics*, edited by D. Bercovici, and G. Schubert, Elsevier, Amsterdam, 2007, pp. 253–303.
3. L. H. Kellogg, B. H. Hager, and R. D. van der Hilst, *Science* **283**, 1881–1884 (1999).
4. F. Albarède, and R. D. van der Hilst, *EOS Transactions American Geophysical Union* **45**, 535–539 (1999).
5. P. J. Tackley, *Science* **288**, 2002–2006 (2000).
6. C. R. Carrigan, *Science* **215**, 956–967 (1982).
7. F. A. Kulacki, and R. J. Goldstein, *J. Fluid Mech.* **271**, 271–287 (1972).
8. D. J. Tritton, and M. M. Zarraga, *J. Fluid Mech.* **30**, 21–31 (1967).
9. E. W. Schwiderski, and H. J. A. Schwab, *J. Fluid Mech.* **48**, 703–717 (1971).
10. R. Krishnamurti, *J. Fluid Mech.* **33**, 445–455 (1968).
11. S. A. Weinstein, and P. Olson, *Geophys. Res. Lett.* **17**, 239–242 (1990).
12. E. Surducan, V. Surducan, C. Neamtu, and C. D. Tudoran, *IEEE International Conference on Automation, Quality and Testing, Robotics* **48**, 360–364 (DOI:10.1109/AQTR.2010.5520760, 2010).
13. V. Surducan, E. Surducan, R. Ciupa, and M. Roman, *IEEE International Conference on Automation, Quality and Testing, Robotics* **48**, 366–371 (DOI:10.1109/AQTR.2010.5520705, 2010).
14. P. J. Tackley, *Geophys. Res. Lett.* **20**, 2187–2190 (1993).
15. L. Rayleigh, *Philosophical Magazine* **32**, 529–546 (1916).
16. A. Davaille, and A. Limare, “Laboratory studies on mantle convection,” in *Treatise of Geophysics*, edited by D. Bercovici, and G. Schubert, Elsevier, Amsterdam, 2007, pp. 89–165.
17. E. Surducan, V. Surducan, and C. Neamtu, *AIP Conference Proceedings* **1425**, 85–88 (2012).
18. A. Davaille, *Journal of Fluid Mechanics* **379**, 223–253 (1999).
19. E. Surducan, C. Neamtu, V. Surducan, A. Limare, and E. di Giuseppe, *AIP Conference Proceedings* **this conference** (2013).
20. D. Dabiri, *Exp Fluids* **46**, 191–241 (2009).
21. A. Davaille, A. Limare, F. Touitou, I. Kumagai, and J. Vatteville, *Exp Fluids* (DOI:10.1007/s00348-010-0924-y, 2010).

This article is copyrighted as indicated in the abstract. Reuse of AIP content is subject to the terms at: http://scitation.aip.org/termsconditions. Downloaded to IP: 194.254.220.140 On: Tue, 19 Nov 2013 08:34:07